RESEARCH ARTICLE

Amyloid Against Amyloid: Dimeric Amyloid Fragment Ameliorates Cognitive Impairments by Direct Clearance of Oligomers and Plaques

HeeYang Lee,[‡[a]] Seungyeop Baek,[‡[a]] Minhae Cha,[‡[a]] Seung-Hoon Yang,[‡[c]] Illhwan Cho,[[a]] Heewon Shin,[[a]] Sejin Lee,[[a]] Hye Yun Kim,[[a]] Songmin Lee,[[a]] Jisu Shin,[[a]] Donghee Lee,[[a]] Kyeonghwan Kim,[[a]] InWook Park,[[a]] Soljee Yoon,[[a,b]] Jiyoon Kim,[[d]] SeongJeong Park,[[f]] Seong Muk Kim,[[f]] Ko Eun Kim,[[f]] Hye Ju Kim,[[f]] Min-Seok Oh,[[e,g]] Gwan-Ho Lee,[[e]] Byung-Yong Yu,[[e]] Priyadharshini Kannan,[[g,h]] Keunwan Park,[[h]] YoungSoo Kim,*[[a,b,f]]

[a] Ms. H. Lee, Dr. S. Baek, Ms. M. Cha, Mr. I. Cho, Ms. H. Shin, Dr. S. Lee, Dr. H.Y. Kim, Ms. S. Lee, Dr. J. Shin, Dr. D. Lee, Mr. K. Kim, Mr. I. Park, Ms. S. Yoon, Professor Y. Kim
Department of Pharmacy and Yonsei Institute of Pharmaceutical Sciences
Yonsei University
Yeonsu-gu, Incheon, 21983, South Korea
E-mail: y.kim@yonsei.ac.kr

[b] Ms. S. Yoon, Professor Y. Kim
Department of Integrative Biotechnology and Translational Medicine
Yonsei University
Yeonsu-gu, Incheon, 21983, South Korea

[c] Professor S-H. Yang
Department of Medical Biotechnology
Dongguk University
Jung-gu, Seoul, 04620, South Korea

[d] Ms. J. Kim
Brain Science Institute
Korea Institute of Science and Technology
Seongbuk-gu, Seoul, 02792, South Korea

[e] Mr. M-S. Oh, Dr. G-H. Lee, Dr. B-Y. Yu
Advanced Analysis and data Center
Korea Institute of Science and Technology
Seongbuk-gu, Seoul, 02792, South Korea

[f] Mr. S. Park, Dr. S.M. Kim, Ms. K.E. Kim, Ms. H.J. Kim
Amyloid Solution
Bundang-gu, Seongnam-si, Gyeonggi-do, 13486, South Korea

[g] Mr. M-S. Oh
Department of Stem Cell Biology
Konkuk University
Gwangjin-Gu, Seoul, 05029, South Korea

[h] Ms. P. Kannan
Department of Biochemical Engineering
Gangneung-Wonju National University
Gangneung, 25457, South Korea

[i] Ms. P. Kannan, Professor K. Park
Natural Product Informatics Research Center
Korea Institute of Science and Technology
Gangwon-do, 25451, South Korea

[‡] These authors contributed equally to this work.

Supporting information for this article is given via a link at the end of the document.

Abstract: Amyloid-β (Aβ) in the form of neurotoxic aggregates is regarded as the main pathological initiator and key therapeutic target of Alzheimer's disease. However, anti-Aβ drug development has been impeded by the lack of a target needed for structure-based drug design and low permeability of the blood-brain barrier (BBB). An attractive therapeutic strategy is the development of amyloid-based anti-Aβ peptidomimetics that exploit the self-assembling nature of Aβ and penetrate the BBB. Herein, we designed a dimeric peptide drug candidate based on the N-terminal fragment of Aβ, DAB, found to cross the BBB and solubilize Aβ oligomers and fibrils. Administration of DAB reduced amyloid burden in 5XFAD mice, and downregulated neuroinflammation and prevented memory impairment in the Y-maze test. Peptide mapping assays and molecular docking studies were utilized to elucidate DAB-Aβ interaction. To further understand the active regions of DAB, we assessed the dissociative activity of DAB with sequence modifications.

Introduction

Amyloid proteins transiently folding into heterogenous aggregates are implicated as the pathological initiators of neurodegenerative disorders.[1] In Alzheimer's disease (AD), amyloid-β (Aβ) spontaneously aggregates into neurotoxic oligomeric and fibrillar assemblies that deposit as amyloid

plaques.[2] Accumulation of Aβ aggregates in the brain initiates pathological downstream cascades contributing to cognitive decline, including the abnormal activation of glial cells, microglia and astrocytes, associated with neuroinflammation and cell death.[3] As such, neurotoxic amyloid aggregates are regarded as a key therapeutic target for AD therapy.

Many attempts to develop disease-modifying drugs targeting amyloid in the brain were made but have seen very little success. Due to the intrinsically unstructured and polymorphic nature of Aβ, the development of Aβ-targeting small molecules is impeded by the lack of a definite target structure needed for rational drug design and resultant off target interactions.[4] Anti-Aβ antibody drugs can overcome target-specificity, but have high production cost and poor drug delivery across the blood-brain barrier (BBB).[5] Peptide-based drugs can be an attractive alternative to small molecules and antibody drugs owing to their high-selectivity, low cost, and BBB permeability.[6] Shifting perspective, an amyloid-based peptide drug exploiting the self-assembling nature of amyloid can best overcome the polymorphic nature of the therapeutic target. Several research groups have evinced the therapeutic efficacy of Aβ-targeting peptide drugs derived from the central hydrophobic core or C-terminal of Aβ.[7]

Recently, clinical AD studies have been recurrently reported the increase of 16-17 residue N-terminal fragments of the full-length Aβ(1-42), Aβ(1-17), in the cerebrospinal fluid of early AD patients.[8] As opposed to the central hydrophobic core or hydrophobic C-terminal, the N-terminal fragment of Aβ is mainly comprised of hydrophilic residues and its anti-amyloid therapeutic potential has not been investigated. In this study, we hypothesized the transient rise of Aβ(1-17) levels may be an innate defense mechanism against amyloid aggregation and assessed its anti-amyloid properties. We found that Aβ(1-17) dissociates aggregates of Aβ(1-42) *in vitro* and designed a dimeric Aβ(1-17)-based peptide drug (DAB) that binds to and solubilizes neurotoxic Aβ aggregates with enhanced multivalency effect (Scheme 1). Upon administration to 5XFAD transgenic mice, DAB crosses the BBB and reduced amyloid burden, concomitantly alleviated neuroinflammation and inhibited memory impairment in the Y-maze test. Furthermore, peptide mapping assays were fabricated and performed to predict binding and dissociation sites of DAB. To assess essential residues for dissociative activity, truncation and lengthening modifications of DAB were performed.

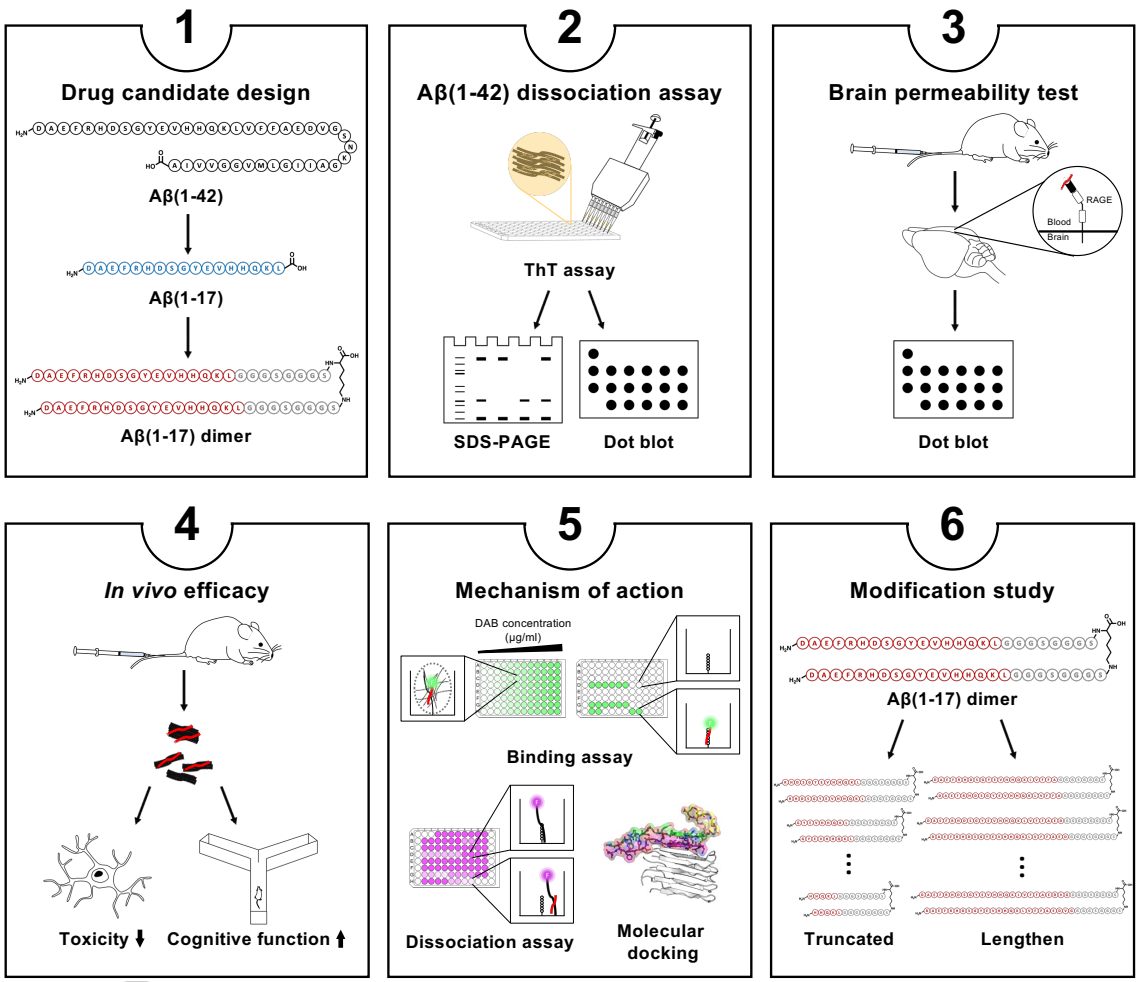

Scheme 1. Scheme of study. 1) Drug candidate, DAB, was designed as a dimeric form of Aβ(1-17). 2) In vitro assays were performed to verify the dissociating ability of DAB against Aβ(1-42) aggregation. 3) Brain permeability tests suggest DAB crosses the BBB via RAGE. 4) Administration of DAB lowered amyloid burden in transgenic Alzheimer mice, concomitantly downregulating inflammatory biomarkers and preventing cognitive decline. 5) Mechanism of action was elucidated by mapping sites of interactions and molecular docking simulations. 6) Modification studies were executed to find critical regions for dissociative activity.

Results and Discussion

Non-amyloidogenic Aβ(1-17) Solubilizes Aggregated Aβ(1-42)

To assess the anti-amyloid properties of the N-terminal fragment of Aβ, we first acquired Aβ(1-17) and Aβ(1-42) peptides through fluorenylmethyloxycarbonyl solid-phase peptide synthesis (Fmoc SPPS) (Figure 1a,; See Figure S1a-d in the Supporting Information). Then we tested whether Aβ(1-17) exhibited self-aggregation characteristic of amyloid proteins by incubating monomeric Aβ(1-17) samples dissolved in 1% DMSO at concentrations of 0.25, 2.5, 25, 125, and 250 μM at 37°C for 24 hours. Monomeric Aβ(1-42) dissolved in 1% DMSO at 25 μM was prepared and incubated for comparison. After 24 hours, Aβ(1-42) aggregated into β-sheet-rich fibrils detected by thioflavin T (ThT) fluorescence, while Aβ(1-17) did not exhibit self-assembly (Figure 1b).

Inhibitory action by Aβ(1-17) against Aβ(1-42) aggregation was assessed by the co-incubation of Aβ(1-17) (0.25, 2.5, 25, 125, and 250 μM) and monomeric Aβ(1-42) (25 μM) at 37°C for 24 hours. Upon measurement of ThT-detected fibrillar content, we found that co-incubation of Aβ(1-17) 250 μM inhibited the formation of aggregated Aβ(1-42) by 40.51% in comparison to Aβ(1-42)-only samples (P < 0.0001) (Figure 1c). Next, dissociative activity of Aβ(1-17) against pre-formed Aβ(1-42) aggregates was evaluated. Aβ(1-42) aggregates were prepared by incubation at 37°C for 24 hours, and were subsequently treated with Aβ(1-17) for an additional 24 hours. At 250 μM, Aβ(1-17) dissociated Aβ(1-42) fibrils by 22.04% (P < 0.0001) (Figure 1d).

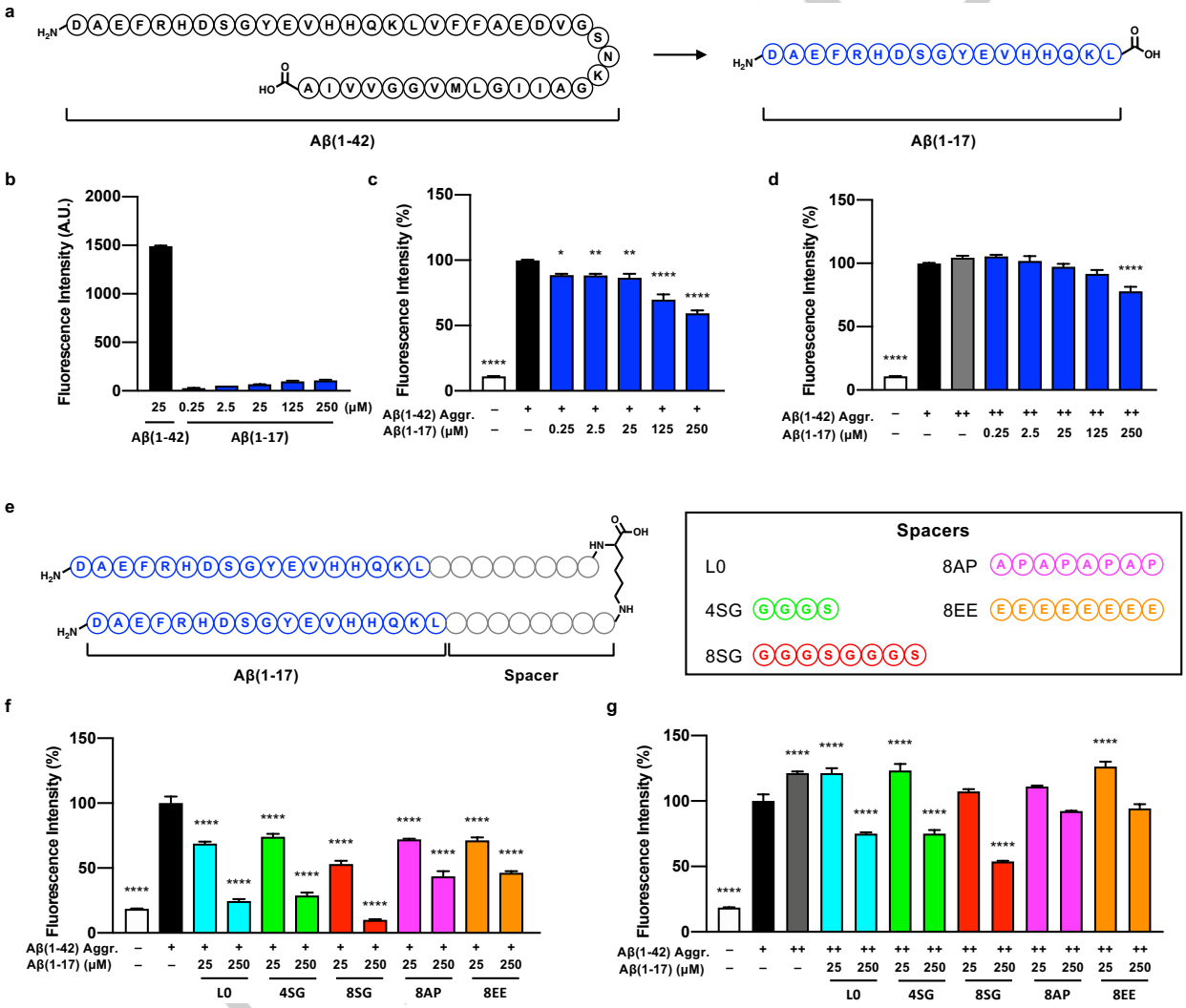

Figure 1. Design of anti-amyloidogenic N-terminal based dimeric Aβ peptide drug. a) Sequence of Aβ(1-42) and N-terminal fragment Aβ(1-17). b) ThT-detected β-sheet fibril content of Aβ(1-42) (25 μM) and Aβ(1-17) (0.25, 2.5, 25, 125, 250 μM) aggregated for 1 day. c) Inhibitory effects of Aβ(1-17) (0.25, 2.5, 25, 125, 250 μM) against Aβ(1-42) (25 μM) aggregation were evaluated using ThT fluorescence. d) Dissociative effects of Aβ(1-17) (0.25, 2.5, 25, 125, 250 μM) against pre-aggregated Aβ(1-42) (25 μM) were evaluated using ThT fluorescence. e) Schematic illustration of spacer selection for dimeric Aβ(1-17)-based peptide drug. f) Inhibitory effects of dimeric Aβ(1-17) with various spacers (L0, 4SG, 8SG, 8AP, and 8EE) against Aβ(1-42) (25 μM) aggregation. g) Dissociative effects of dimeric Aβ(1-17) with various spacers (L0, 4SG, 8SG, 8AP, and 8EE) against pre-aggregated Aβ(1-42) (25 μM). Total aggregation time for Aβ(1-42) is indicated as '–' for 0 day, '+' for 1 day, and '++' for 2 days. Fluorescence intensities for inhibition and dissociation assays were normalized and statistically compared to Aβ(1-42)-only 1 days (+) control (100%). One-way analysis of variance followed by Bonferroni's post-hoc comparisons tests were performed in all statistical analyses (*P < 0.05, **P < 0.01, ****P < 0.0001). Data are presented as mean ± SEM. Abbreviations: Aggr. = Aggregation.

Design of Dimeric Aβ(1-17)-based Peptide

As our results suggested that Aβ(1-17) is a non-amyloidogenic fragment that possesses anti-amyloid properties against Aβ(1-42) aggregation, we sought to design a Aβ(1-17)-based peptide drug candidate. To enhance the Aβ-solubilizing abilities of Aβ(1-17), we attached two peptide fragments by using lysine amine groups as a linker and added spacers to increase accessibility and flexibility. For optimal spacer selection, we tested the inhibitory and dissociative activity of a dimer with no spacer (L0) and dimers with four types of spacers: 4SG (GGGS), 8SG (GGGSGGGS), 8AP (APAPAPAP), and 8EE (EEEEEEEE) (Figure 1e; See Figure S2a-j). Dimeric fragments attached with 8SG spacers had the highest efficacy in ThT assays testing for Aβ(1-42) aggregate inhibition (Figure 1f) and dissociation (Figure 1g). Additionally, 8SG linker, dimeric form of 8SG spacers, solely is insufficient to create the effect that dimeric fragments attached with 8SG spacers exert (See Figure S3a-d) and may enhance the solubilizing effect of the dimeric fragments. Thus, 8SG spacers attached dimer fragments form was selected for DAB sequences.

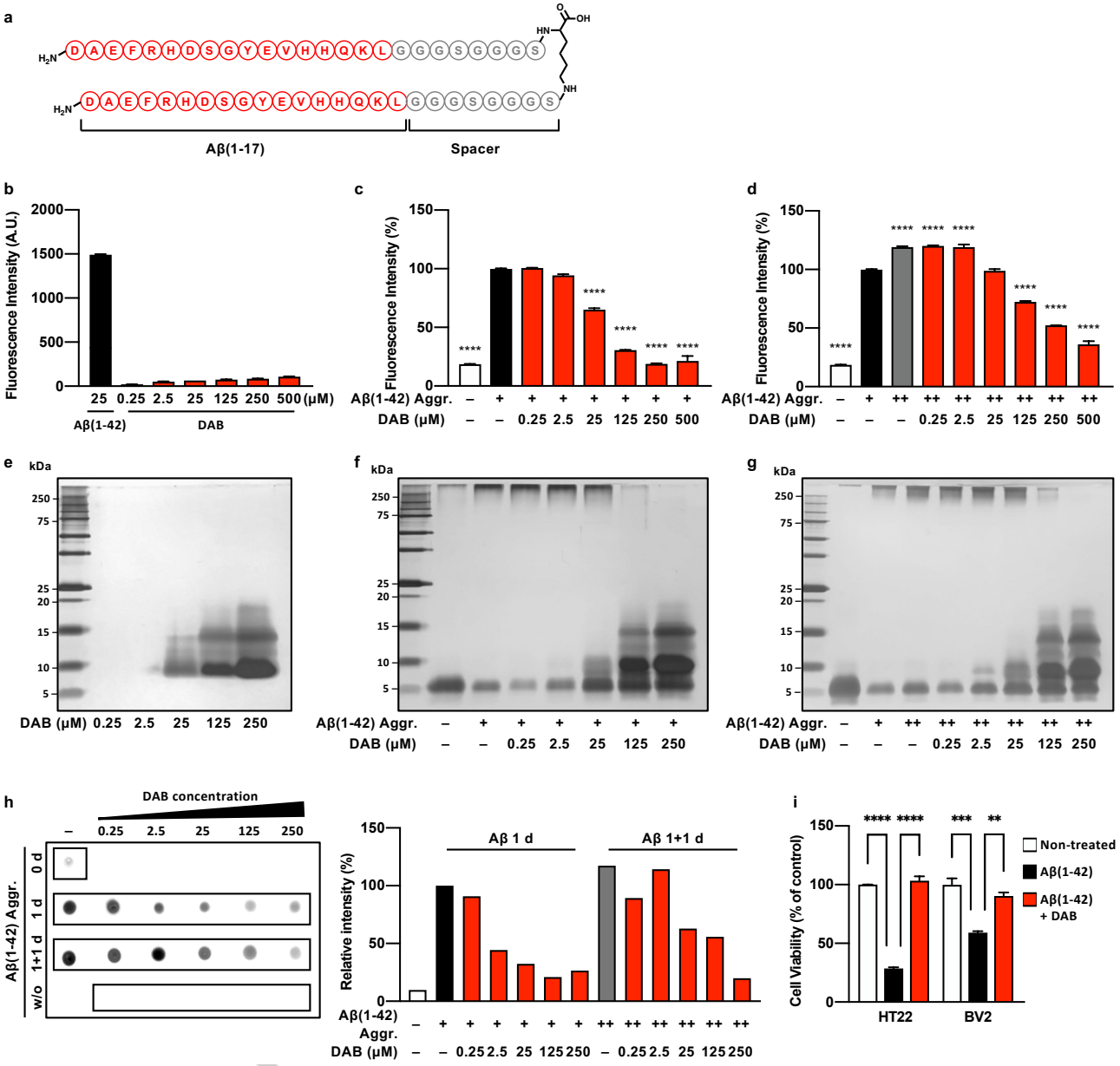

Figure 2. DAB solubilizes toxic amyloid fibrils and oligomers. a) Sequence of DAB, a dimeric Aβ(1-17) peptide drug. b) ThT-detected β-sheet fibril content of Aβ(1-42) (25 μM) and DAB (0.25, 2.5, 25, 125, 250, 500 μM) aggregated for 1 day. ThT fluorescence assay of c) inhibitory effects and d) dissociative effects of DAB (0.25, 2.5, 25, 125, 250, 500 μM) against Aβ(1-42) (25 μM) aggregation. Gel electrophoresis with PICUP and silver staining of e) DAB only, f) DAB-inhibited Aβ(1-42) species, and g) DAB-dissociated Aβ(1-42) species. h) Dot blot assay using anti-oligomeric A11 antibody to detect oligomeric species of DAB (lower row), DAB-inhibited Aβ(1-42) species (higher row), and DAB-dissociated Aβ(1-42) (middle row) with respective densitometries. i) Aβ(1-42)-induced toxicity was reduced upon co-incubation of Aβ(1-42) (10 μM) with DAB (10 μM) in HT22 and BV2 cell lines for 24 hours. Total aggregation time for Aβ(1-42) is indicated as '–' for 0 day, '+' for 1 day, and '++' for 2 days. Fluorescence intensities for inhibition and dissociation assays were normalized and statistically compared to Aβ(1-42)-only 1 days (+) control (100%). One-way analysis of variance followed by Bonferroni's post-hoc comparisons tests were performed in all statistical analyses (**P < 0.01, ***P < 0.001, ****P < 0.0001). Data are presented as mean ± SEM. Abbreviations: Aggr. = Aggregation.

DAB Dissociates Neurotoxic Aβ(1-42) Oligomers and Fibrils

The sequence of the DAB selected for this study is shown in Figure 2a (See Figure S4a-d). To check for self-assembly, DAB was dissolved in 1% DMSO at concentrations of 0.25, 2.5, 25, 125, 250, and 500 μM and incubated at 37°C for 24 hours. Similar to Aβ(1-17), DAB did not exhibit self-assembly into β-sheet-rich aggregates (Figure 2b). Co-incubation of DAB with Aβ(1-42) monomers inhibited the formation of ThT-detected Aβ(1-42) fibrils by 81.05% at 250 μM ($P < 0.0001$) and by 78.59% at 500 μM ($P < 0.0001$) (Figure 2c). In the dissociation assay, DAB disaggregated fibrils by 47.68% at 250 μM ($P < 0.0001$) and by 63.94% at 500 μM ($P < 0.0001$) (Figure 2d), exhibiting higher solubilizing ability than Aβ(1-17) against aggregated Aβ(1-42).

Through gel electrophoresis followed by silver staining, DAB at concentrations of 25, 125, and 250 μM could be seen at 8 kDa and as dimers at 16 kDa but not fibrils (Figure 2e). The monomeric and fibril forms of Aβ(1-42) aggregates treated with DAB were separated and visualized by gel electrophoresis followed by silver staining. Prior to gel analysis, metastable DAB and Aβ(1-42) assemblies were fixed by photoinduced crosslinking of unmodified proteins (PICUP). In inhibition assay samples, fibrillar Aβ(1-42) assemblies at high molecular weights (~250 kDa) were effectively reduced in 125 μM and 250 μM, with concomitant increase of monomeric species at 4.2 kDa (Figure 2f). In dissociation assay samples, DAB 250 μM markedly reduced fibrils while increasing monomers (Figure 2g). The oligomeric levels of Aβ(1-42) samples were quantified by dot blot assay utilizing the anti-oligomer A11 antibody (Figure 2h). DAB at higher concentrations reduced blot intensity of A11-detected Aβ(1-42) and the oligomeric species of DAB (lower row in Figure 2h) were not detected. Our results suggest that the co-incubation of DAB solubilizes both oligomeric and fibrillar species of Aβ(1-42) to monomeric states.

As aggregates of Aβ(1-42) exert neurotoxic effects characteristic of AD pathology, we tested whether solubilization of aggregates by DAB could reduce Aβ-induced cell toxicity utilizing MTT assay. Prior to assessing anti-Aβ toxicity, we examined whether DAB had innate toxicity. DAB at concentrations of 2000, 1000, 500, 250, 124, 61.5, and 31.25 μM was treated to HT22 cells for 24 hours and subsequently MTT reagent was utilized to quantify cell viability (See Figure S5). Our results show that the TD_{50} of DAB in HT22 cells was higher than 2000 μM, suggesting DAB has low toxicity. Next, we assessed if the co-treatment of DAB could alleviate Aβ neurotoxic effects. Aβ(1-42) treatment of 24 hours significantly induced cell death in HT22 cells and BV2 cells, and co-incubation of DAB significantly prevented Aβ-induced neurotoxicity (Figure 2i). In sum, our results show that DAB solubilizes Aβ(1-42) aggregates and prevents Aβ-induced toxicity.

DAB Reduced Amyloid Burden and Rescues Aβ-induced Memory Deficits and Inflammation in 5XFAD Mice

The therapeutic efficacy of DAB against Aβ was evaluated in the 5XFAD, a transgenic AD mouse model with aggressive amyloid accumulation. Adult models of AD and aged models of AD were selected at the ages of 5 months and 11 months, respectively (Figure 3a). During an administration period of five weeks, DAB (200 mg/kg) was dissolved in PBS (See Figure S6) and intravenously injected to adult model 5XFAD mice three times per week. Age- and sex-matched littermate wildtype and 5XFAD mice were injected PBS as controls. During the last week of DAB administration, we assessed changes in hippocampal memory impairment of the mice at the age of 6 months by employing the Y-maze test. In addition, untreated 5-month-old male wildtype and 5XFAD mice were used as pre-treatment controls. While PBS-injected 5XFAD mice displayed significant decrease of spontaneous alternations in comparison to wildtype mice, DAB-treated mice increased the alternation levels to wildtype level (Figure 3b). Total arm entries were not different among groups (Figure 3c) and representative tracking heatmaps of the aged model groups are shown in Figure 3d. After five weeks, the mice were sacrificed, and brains were extracted for protein analysis. As the hippocampus is one of the earliest brain areas affected in AD,[9] the alterations of hippocampal Aβ levels were examined through western blot analysis (See Figure S7). In comparison to PBS-treated 5XFAD mice, Aβ oligomers were lowered by 21.46% in DAB-treated mice ($P < 0.05$) (Figure 3e). Furthermore, in DAB-treated mice, astrogliosis detected by anti-GFAP and microglial activation detected by anti-Iba1 were inhibited by 17.62% ($P < 0.05$) and 24.05% ($P < 0.05$), respectively (Figure 3e).

Next, we assessed the dissociative ability of DAB against Aβ aggregates in the aged models of mice manifesting abundant deposits of amyloid plaques. DAB (200 mg/kg) was treated to 11-month-old 5XFAD mice for 2 weeks, three times a week, via intravenous injections. Control 5XFAD mice were injected PBS. After 2 weeks, the brains were extracted and dissected in to two hemispheres for immunohistochemical staining and western blot analysis. In the aged models, DAB treatment reduced the number of plaques in the hippocampus and whole brain slides by 50.09% ($P < 0.01$) and 31.64% ($P < 0.01$), respectively (Figure 3, f-h). In hippocampal lysates, levels of oligomeric Aβ and Iba1 were lowered by 34.52% ($P < 0.05$) and 24.97% ($P < 0.01$), while a trend of decline was observed in GFAP (reduced by 12.21%, $P = 0.0746$) (Figure 3i).

DAB Crosses the BBB via RAGE-mediated Transport

Injection of DAB to 5XFAD mice reduced amyloid burden in the brain, suggesting that DAB crosses the BBB. To confirm that DAB enters the brain, we prepared and administered ^{14}C-methylated-DAB to wildtype mice via intravenous injections, and subsequently examined the time-dependent concentration of DAB in the plasma and brain (Figure 4a; See Figure S8). ^{14}C-methylated-DAB was found in the plasma and brain at highest concentrations at 20 minutes, 3694.5 ng/mL and 2353.2 ng/g, respectively, and showed time-dependent decrease in concentration (Figure 4b). The brain to plasma ratio was 0.65 at 20 minutes, 0.80 at 40 minutes, and 1.07 at 60 minutes (Table 1), confirming that DAB crosses the BBB. Furthermore, we assessed the concentration and total amount of ^{14}C-methylated-DAB in the cerebral cortex, hippocampus, cerebellum, olfactory bulb, and remaining regions (Figure 4c, d).

Table 1. Brain to plasma ratio of [C14] methyl DAB in mice.

Time (min)	Brain (ng/g)	Plasma (ng/mL)	Brain to Plasma Ratio
20	2353.2	3694.5	0.65
40	2013.0	2489.7	0.80
60	1542.6	1361.2	1.07

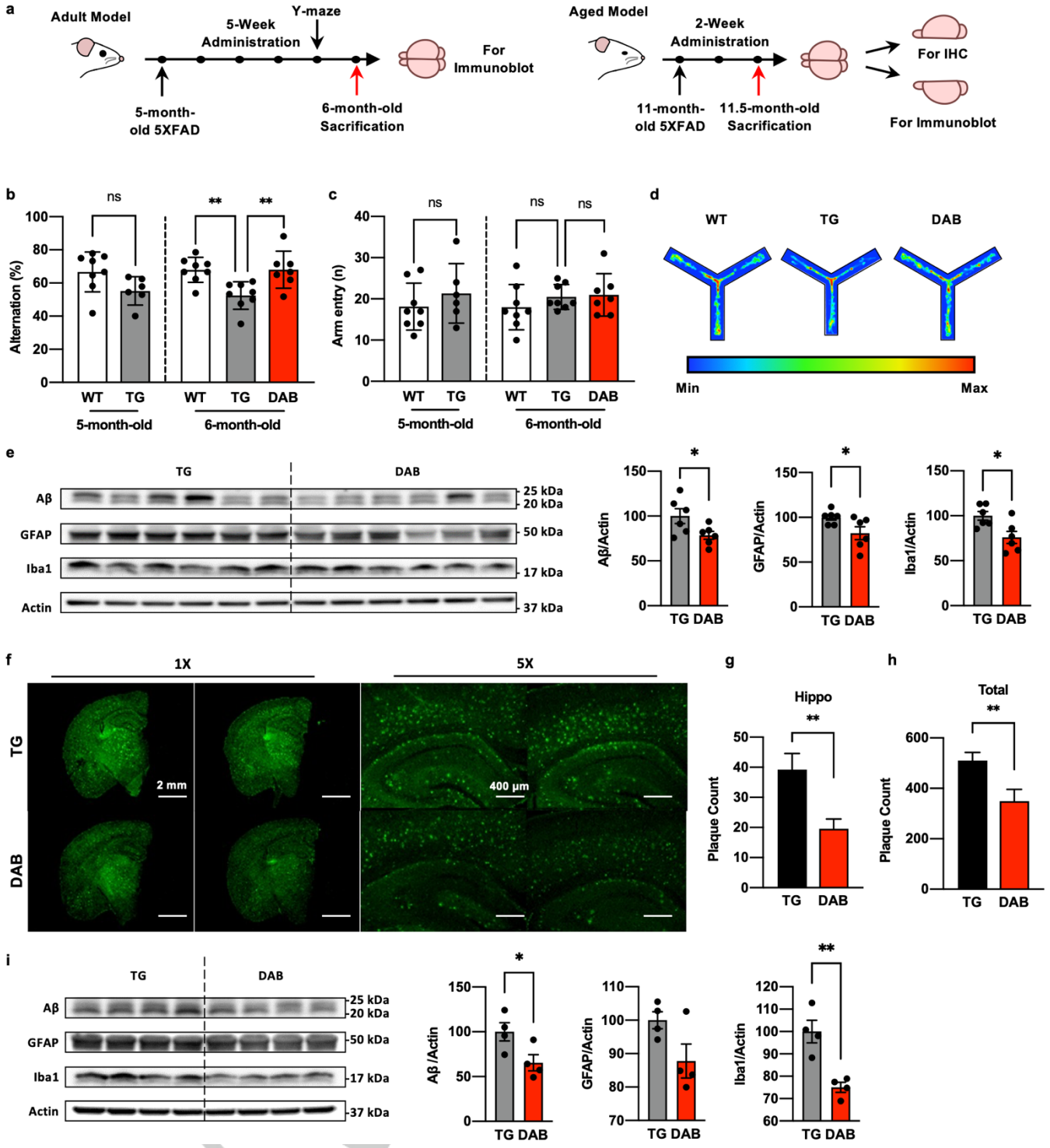

Figure 3. DAB reduces Aβ plaques and oligomers in 5XFAD mice, rescuing hippocampal memory and alleviating neurotoxicity. a) Scheme of DAB administration to adult and aged AD mouse models. b-e) DAB (200 mpk) was administered via IV injection to 5-month-old male 5XFAD mice for 5 weeks. b) Spontaneous alternation and c) total entry in Y-maze test for pretreated 5-month-old mice and treated 6-month-old mice. d) Representative heatmap of Y-maze trials. e) Through western blot, soluble fractions of hippocampal lysates of the 6-month-old were immunoblotted for Aβ oligomers, GFAP, and Iba1, with respective densitometries. f-i) DAB (200 mpk) was administered via IV injection to 11-month-old male 5XFAD mice for 2 weeks. f) Brains were immunostained with 6E10 (green) and the number of plaques in the g) hippocampus and h) total slice of the mice were quantified. i) Through western blot, soluble fractions of hippocampal lysates of the 11.5-month-old mice were immunoblotted for Aβ oligomers, GFAP, and Iba1, with respective densitometries. Densitometries were normalized and statistically compared to PBS-treated 5XFAD mice (100%). Two-tailed T-tests and one-way analysis of variance followed by Bonferroni's post-hoc comparisons tests were performed for statistical analyses (*$P < 0.05$ and **$P < 0.01$). Data are presented as mean ± SEM.

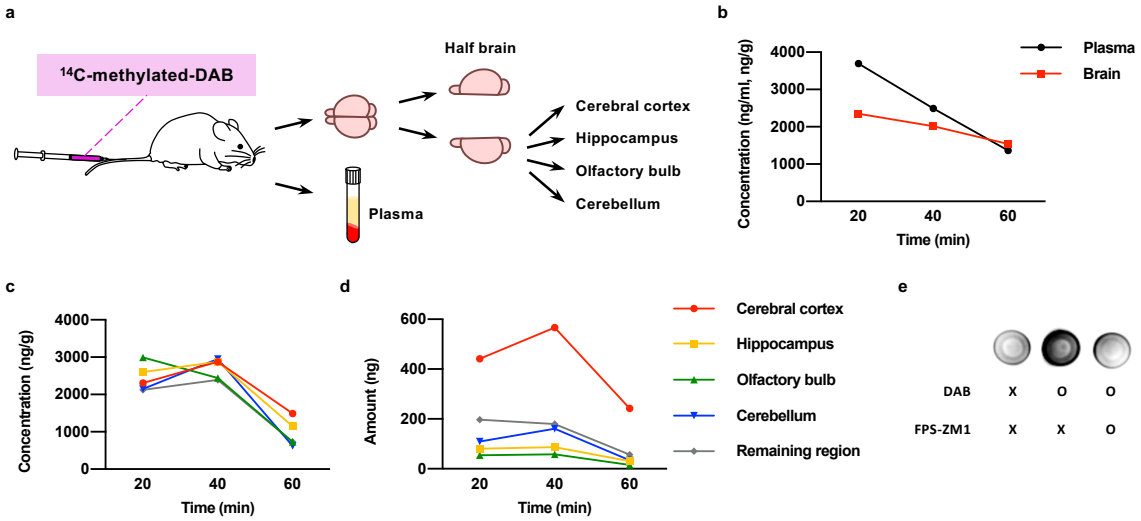

Figure 4. DAB crosses the BBB. a) ^{14}C-methylated-DAB was synthesized and administrated to wildtype mice. b) Concentration of ^{14}C-methylated-DAB in the plasma (ng/mL) and whole brain (ng/g). c) Concentration of ^{14}C-methylated-DAB in specific brain regions (ng/g). d) Total amount of ^{14}C-methylated-DAB in specific brain regions (ng). e) Entry of DAB is blocked upon inhibition of RAGE transporter in wildtype mice.

Aβ is well known to enter the brain from the blood by receptor for advanced glycation endproducts (RAGE),[10] but the exact mechanism has not been elucidated. A molecular modeling study predicted that the N-terminal of Aβ interacts with RAGE, which transports Aβ from the blood to the brain.[11] To test whether RAGE transports DAB across the BBB, we injected DAB (200 mg/kg) to wildtype mice treated with RAGE inhibitor FPS-ZM1 (1 mg/kg) and extracted their brain after 20 minutes. As controls, we injected PBS and DAB (200 mg/kg) to wildtype mice. Brain lysates were blotted onto membranes and probed with anti-6E10 antibody, which detects Aβ residues 1-16. We found that DAB-injected mice had higher intensity in comparison to PBS-injected mice and DAB-injected mice treated with RAGE-inhibitor (Figure 4e). Our results suggest that RAGE, at least in part, contributes to the transport of DAB across the BBB.

Binding Site and Dissociation Site of DAB

We then investigated whether DAB dissociates Aβ aggregates through direct binding. To test this possibility, we fabricated Aβ aggregate plates. Aβ(1-42) peptides with terminal cysteine residues were synthesized by Fmoc SPPS and immobilized to a maleimide activated well plate, which was subsequently incubated with monomeric Aβ(1-42) (10 μM) for 24 hours to create aggregates. To test for concentration-dependent binding, DAB labeled by fluorescent dye fluorescein-5-isothiocyanate (FITC) (10 μM) was synthesized and added to the wells in a range of concentrations (0.005, 0.01, 0.05, 0.1, 0.5, 1, 5, 10, 50, 100, 500, 1000, and 5000 μg/mL). A blank well was used as a control. After 20 minutes, we measured the fluorescence intensity of the wells and found DAB exhibited concentration-dependent binding to Aβ(1-42) aggregates, suggesting direct interaction (Figure 5a, b).

As our results suggest DAB directly binds to Aβ, we sought to identify both the binding site and dissociation site involved in interactions between DAB and Aβ by utilizing an Aβ-fragment-based mapping assays. Sequential Aβ fragments of 6 residues with terminal cysteine residues were synthesized by Fmoc SPPS and immobilized to a maleimide activated well plate. A blank well and full-length Aβ(1-42)-bound well were prepared as controls.

To identify the binding site of interaction between DAB and Aβ, DAB labeled by FITC (10 μM) was synthesized and incubated in the wells of the mapping plate for 24 hours (Figure 5c). For comparison, we prepared and incubated FITC-labeled Aβ(1-17) in separate wells. After 24 hours, wells with binding sequences exhibited enhanced fluorescence intensity. Aβ(1-17) and DAB bound to full-length Aβ(1-42) sequences with equal strength, but differed in degrees of binding to specific sequences (Figure 5d). DAB exhibited binding preference to Aβ residues 14-19, 15-20, 16-21, the central hydrophobic core, and 37-42, the hydrophobic C-terminal, and weak binding to residues 30-35, the secondary central region.[12] In contrast, Aβ(1-17) displayed moderate binding strength to the three hydrophobic regions, with a slight preference for the C-terminal of Aβ.

Next, to identify the dissociate sites of interaction on Aβ, fluorescently labeled Flamma552-Aβ(1-42) (10 μM) was prepared and incubated in wells for 6 hours to induce aggregates between fluorescent Flamma552-Aβ(1-42) and Aβ fragments (Figure 5e). Fluorescence intensity were measured to establish baselines of individual wells and compared with altered baselines upon incubation of Aβ(1-17) or DAB (500 μM) for 24 hours. Reduced fluorescence intensity in wells were determined as sequences disrupted Aβ(1-42)-Aβ fragment complexes. We found that DAB had stronger dissociation than Aβ(1-17) against full-length Aβ(1-42), and contrasting sites of dissociation (Figure 5f). While Aβ(1-17) dissociated sequences of the central hydrophobic core, DAB dissociated the secondary central region and, with higher strength, the C-terminal of Aβ.

Although the main sites of binding and dissociation by DAB and Aβ(1-17) overlapped, the degree of binding and dissociation differed, implicating that Aβ(1-17) and DAB are distinct entities with differing mechanisms of action. Our results suggest that DAB binds to the central hydrophobic core KLVFF, known as the self-recognition 'nucleation' site of Aβ,[13] and dissociates aggregates at the C-terminal, a critical region for oligomer formation.[14]

DAB Preferential Binds to Aβ(1-42) Aggregates than Monomers

We performed a docking study to examine the interactions between DAB and different aggregated forms of Aβ(1-42) available in the Protein Data Bank (PDB). The single monomeric Aβ(1-42) structure mainly consists of helical motifs while all other Aβ(1-42) aggregates are composed of β-sheets. The constrained docking simulation suggests that the binding complex models display a significant binding energy difference between monomeric and aggregated forms of Aβ(1-42), which strongly suggests that the DAB preferentially binds the aggregated form of Aβ(1-42) rather than the monomeric form (Table S1). The binding mode comparison for the monomeric (PDB ID: 1IYT) and

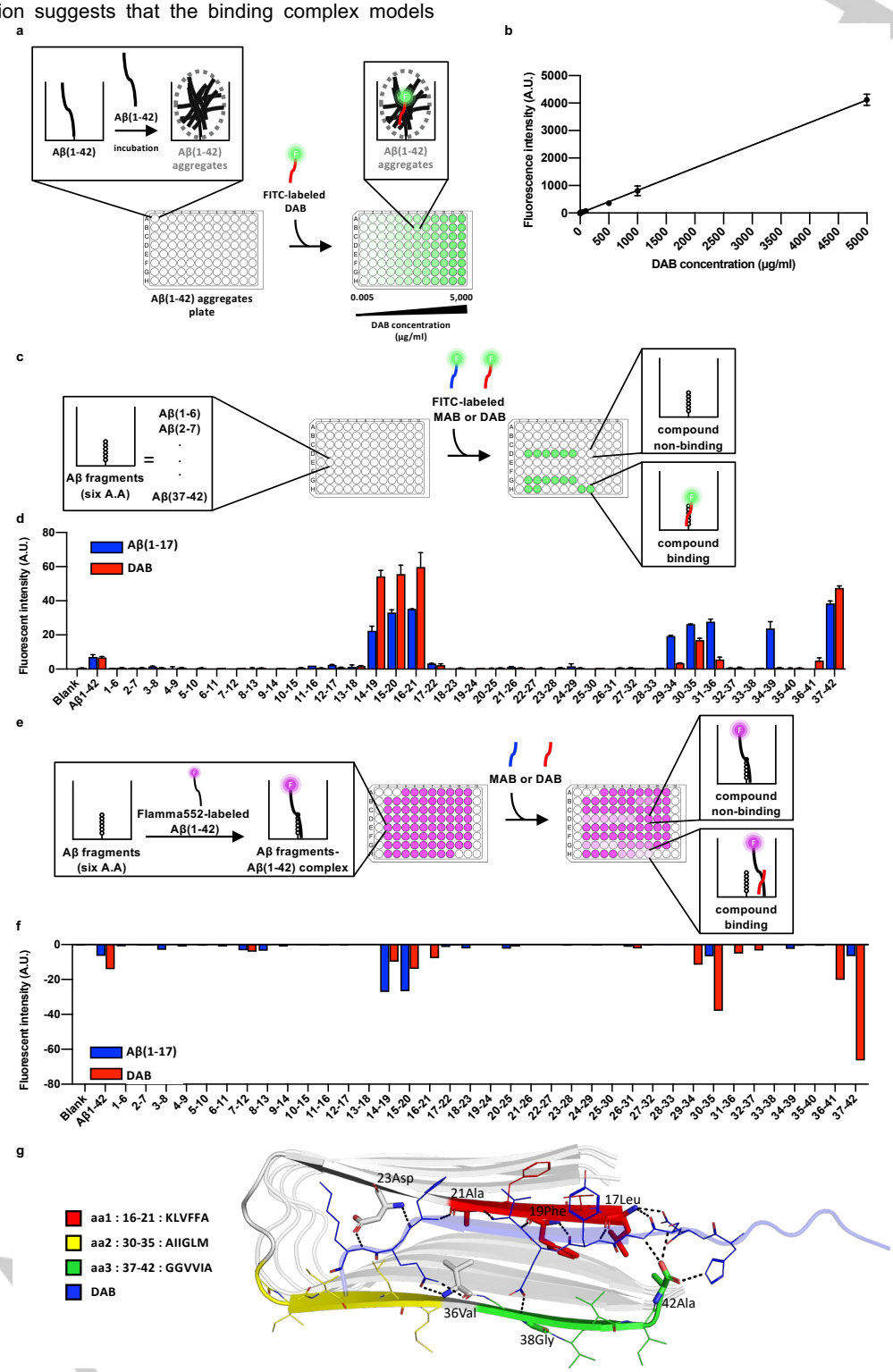

Figure 5. Aβ(1-17) and DAB distinctly bind to and dissociate Aβ. a) Fabrication of concentration-dependent binding assay utilizing well-bound Aβ(1-42) aggregates and FITC-labeled DAB. b) Concentration-dependent binding of DAB to Aβ(1-42) aggregates. c) Fabrication of binding site mapping assay utilizing well-bound hexameric fragments of Aβ and FITC-labeled Aβ(1-17) and DAB. d) Binding sites of Aβ(1-17) and DAB on Aβ were mapped. e) Fabrication of dissociation site mapping assay utilizing Flamma552-labeled Aβ(1-42) aggregated to well-bound hexameric Aβ fragments. f) Dissociation sites of Aβ(1-17) and DAB on Aβ were mapped. g) Binding of DAB to U-shaped aggregated Aβ(1-42).

the representative U-shaped aggregated form (PDB ID: 2BEG) shows distinctive peptide binding modes (Fig. 5g; See Figure S9a-d). In the 2BEG docking model, DAB forms a continuous parallel β-strand (9-14) with the edge strand of Aβ(1-42), which contributes to make a more stable binding complex. Other aggregated Aβ(1-42) structures also showed similar β-strand pairing with DAB. In contrast, DAB was fully exposed and showed little contact with the monomeric Aβ(1-42) 1IYT docking model.

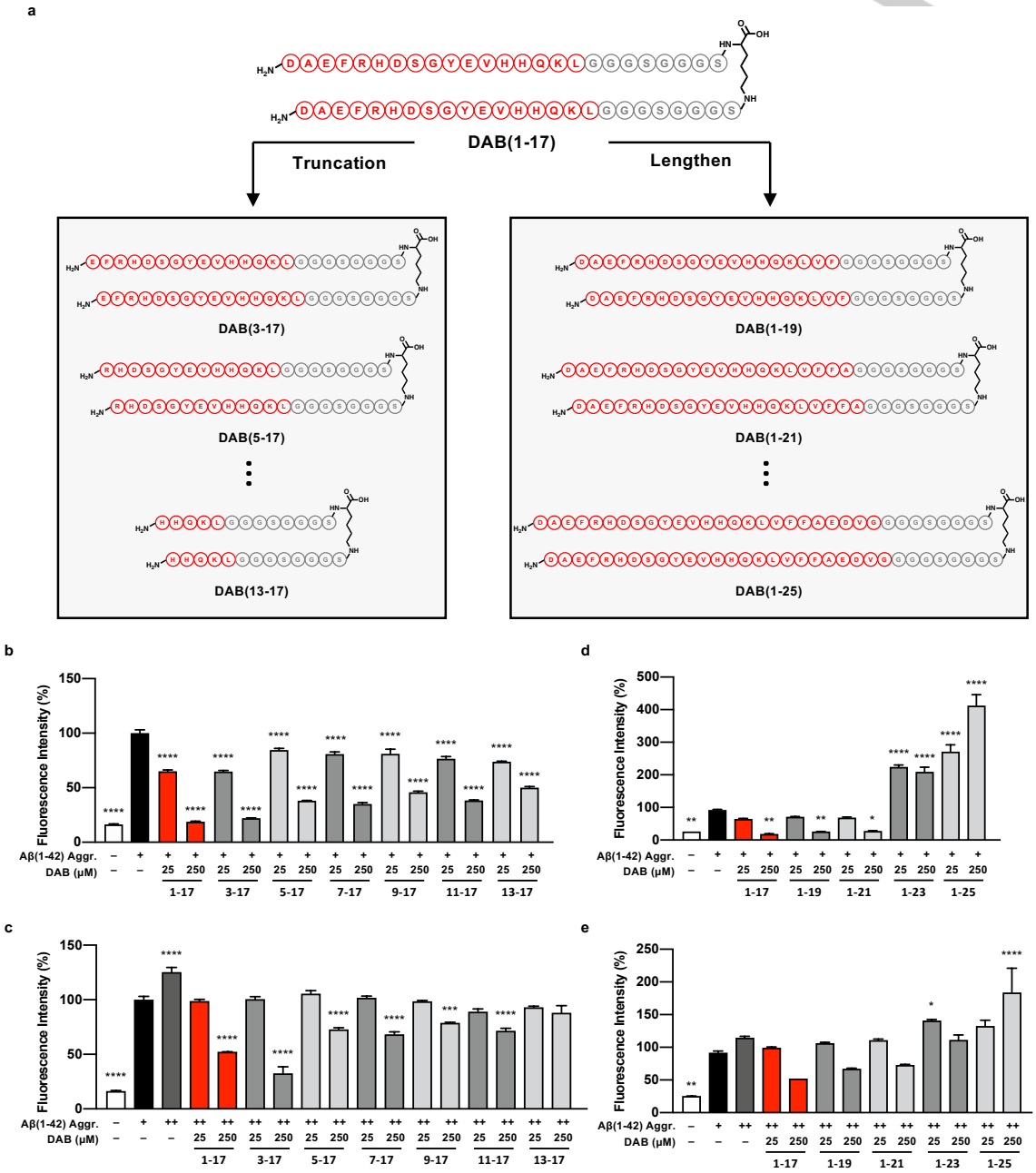

Figure 6. Modification of DAB sequence length. a) DAB with modified sequence lengths were synthesized for dissociative activity analysis. b) Inhibitory effects of DAB with truncated N-terminal against Aβ(1-42) (25 μM) aggregation. c) Dissociative effects of DAB with truncated N-terminal against pre-aggregated Aβ(1-42) (25 μM). d) Inhibitory effects of DAB with lengthened C-terminal against Aβ(1-42) (25 μM) aggregation. e) Dissociative effects of DAB with lengthened C-terminal against pre-aggregated Aβ(1-42) (25 μM). Total aggregation time for Aβ(1-42) is indicated as '–' for 0 day, '+' for 1 day, and '++' for 2 days. Fluorescence intensities for inhibition and dissociation assays were normalized and statistically compared to Aβ(1-42)-only 1 days (+) control (100%). One-way analysis of variance followed by Bonferroni's post-hoc comparisons tests were performed in all statistical analyses (*P < 0.05, **P < 0.01, ***P < 0.001, ****P < 0.0001). Data are presented as mean ± SEM. Abbreviations: Aggr. = Aggregation.

Dissociative Activity of Sequence Modified DAB

Based on clinical reports of the emergence of Aβ(1-17) in early AD, we predicted the therapeutic potential of the 17 N-terminal residues and designed DAB based on the unmodified Aβ(1-17) sequence. To acquire insight to which sequences contribute to the dissociative action of DAB, we synthesized DAB with modified sequence lengths and assessed their anti-Aβ properties. Modified DAB was prepared by truncation by 2 resides at the N-terminal or lengthening by 2 residues at the C-terminal (Figure 6a; See Figure S10a-l and Figure S11a-h). Inhibitory action by DAB gradually decreased as N-terminal residues were truncated (Figure 6b) and the dissociative action was dramatically

decreased after the truncation of 4 residues (Figure 6c). In lengthened versions, inhibitory and dissociative activity of DAB was reduced as the length of sequences increased until the addition of 6 residues, in which DAB(1-23) and DAB(1-25) significantly seeded the aggregation of β-sheet-rich fibrils (Figure 6d,e). Our results suggest that further lengthening of sequences nor truncations exceeding 4 residues do not improve therapeutic potential of DAB.

Conclusion

In this study, we designed an anti-Aβ peptide drug DAB comprising dimeric fragments of Aβ(1-17), which was found to preferentially bind and solubilize amyloid aggregates, and proved its therapeutic efficacy *in vitro* and *in vivo*. Upon administration to the 5XFAD mouse model, DAB reduced Aβ oligomers and plaques, subsequently downregulating neuroinflammation and rescuing cognitive impairment in the Y-maze test. In peptide mapping assays, DAB was shown to bind and dissociate Aβ aggregates in a manner distinct to the Aβ(1-17) fragment. DAB modification studies were conducted to identify residues critical for dissociative activity against aggregates.

Amyloidogenic processing of the amyloid precursor protein (APP) by β-secretase and γ-secretase generates Aβ, while non-amyloidogenic processing involved the α-secretase and γ-secretase.[15] Consecutive cleavage by the α-secretase and β-secretase, a well less known route of APP processing, as well as proteolytic degeneration of Aβ by the matrix metalloproteinase-9 is known to generate Aβ(1-17) fragments, which are increased in the brains of early AD patients.[8a, 16] While peptide drugs based on the hydrophobic core and C-terminal sequences of Aβ have been reported for their dissociative activity,[7] the anti-amyloid properties of the N-terminal fragment of Aβ have not been elucidated. Here, we demonstrated that the N-terminal fragment of Aβ(1-17) can solubilize aggregates of Aβ and have therapeutic potential as a structural basis for anti-amyloid peptide drugs.

Neurotoxicity of Aβ aggregates is reported to initiate multiple pathological cascades characteristic of AD pathology, including neuroinflammation.[17] The administration of DAB reduced both amyloid burden and Aβ-associated microglia and astrocyte activation in adult and aged models of 5XFAD mice. Downregulation of gliosis by DAB may be the result of reduced levels of Aβ oligomers and plaques, and in part, the inhibition of toxic Aβ-microglia interactions via HHQK residues, the microglial-binding domain of Aβ.[18]

The aim of this study is to show the therapeutic potential of anti-amyloid peptide drugs comprising amyloid fragments with solubilizing residues. The dimeric design of DAB did not simply double the dissociative activity of Aβ(1-17), but instead converted DAB into a different entity with substantially enhanced dissociation and distinct interactions. However, we emphasize that DAB is not a drug, but rather a prototype in need of further investigation. Future studies on finding residues involved in RAGE-mediated BBB penetration, optimization studies, and D-form modification are anticipated prior to development as a drug. Our results suggest that dimeric drug design comprising solubilizing and BBB-penetrating sequences may increase the efficacy for peptide drugs targeting other amyloidogenic proteins. As amyloid proteins such as tau, α-synuclein, and prion proteins are reported to cross the BBB,[19] identification and utilization of innate BBB-crossing sequences may facilitate drug delivery to the brain.

Acknowledgements

This research was supported by the Korea Health Technology R&D Project (Grant Number: HU21C0161, Y.K.) through the Korea Health Industry Development Institute (KHIDI) and Korea Dementia Research Center (KDRC), and Mid-Career Researcher Program (Grant Number: NRF-2021R1A2C2093916, Y.K.; NRF-2021R1A2C1013247, H.K.), and Basic Science Research Program (Grant Number: NRF-2018R1A6A1A03023718, Y.K. and H.K.) through the National Research Foundation of Korea (NRF), funded by the Ministry of Health & Welfare and Ministry of Science and ICT, Republic of Korea. This research was also supported by Amyloid Solution, POSCO Science Fellowship of POSCO TJ Park Foundation, and Korea Institute of Science and Technology intramural research grant (K.P.).

Keywords: Alzheimer's disease (AD) • Amyloid-β (Aβ) • Peptide drug

[1] C. A. Ross, M. A. Poirier, *Nat. Med.* **2004**, *10 Suppl*, S10-17.
[2] G.-f. Chen, T.-h. Xu, Y. Yan, Y.-r. Zhou, Y. Jiang, K. Melcher, H. E. Xu, *Acta Pharmacol. Sin.* **2017**, *38*, 1205-1235.
[3] T. Guo, D. Zhang, Y. Zeng, T. Y. Huang, H. Xu, Y. Zhao, *Mol. Neurodegener.* **2020**, *15*, 40.
[4] M. Fändrich, S. Nyström, K. P. R. Nilsson, A. Böckmann, H. LeVine III, P. Hammarström, *J. Intern. Med.* **2018**, *283*, 218-237.
[5] W. M. Pardridge, *Pharmaceuticals (Basel)* **2020**, *13*.
[6] V. Armiento, A. Spanopoulou, A. Kapurniotu, *Angew. Chem., Int. Ed.* **2020**, *59*, 3372-3384.
[7] D. Goyal, S. Shuaib, S. Mann, B. Goyal, *ACS Comb. Sci.* **2017**, *19*, 55-80.
[8] aV. Pérez-Grijalba, P. Pesini, J. A. Allué, L. Sarasa, M. Montañés, A. M. Lacosta, D. Casabona, I. San-José, M. Boada, L. Tárraga, A. Ruiz, M. Sarasa, *J. Alzheimers Dis.* **2015**, *43*, 47-56; bE. Portelius, H. Zetterberg, R. A. Dean, A. Marcil, P. Bourgeois, M. Nutu, U. Andreasson, E. Siemers, K. G. Mawuenyega, W. C. Sigurdson, P. C. May, S. M. Paul, D. M. Holtzman, K. Blennow, R. J. Bateman, *J. Alzheimers Dis.* **2012**, *31*, 335-341.
[9] J. Barnes, J. L. Whitwell, C. Frost, K. A. Josephs, M. Rossor, N. C. Fox, *Arch. Neurol.* **2006**, *63*, 1434-1439.
[10] R. Deane, S. Du Yan, R. K. Submamaryan, B. LaRue, S. Jovanovic, E. Hogg, D. Welch, L. Manness, C. Lin, J. Yu, H. Zhu, J. Ghiso, B. Frangione, A. Stern, A. M. Schmidt, D. L. Armstrong, B. Arnold, B. Liliensiek, P. Nawroth, F. Hofman, M. Kindy, D. Stern, B. Zlokovic, *Nat. Med.* **2003**, *9*, 907-913.
[11] M. O. Chaney, W. B. Stine, T. A. Kokjohn, Y. M. Kuo, C. Esh, A. Rahman, D. C. Luehrs, A. M. Schmidt, D. Stern, S. D. Yan, A. E. Roher, *Biochim. Biophys. Acta* **2005**, *1741*, 199-205.
[12] L. Triguero, R. Singh, R. Prabhakar, *J. Phys. Chem. B* **2008**, *112*, 2159-2167.
[13] T. L. Lowe, A. Strzelec, L. L. Kiessling, R. M. Murphy, *Biochemistry* **2001**, *40*, 7882-7889.
[14] S. Yun, B. Urbanc, L. Cruz, G. Bitan, D. B. Teplow, H. E. Stanley, *Biophys. J.* **2007**, *92*, 4064-4077.
[15] Y.-w. Zhang, R. Thompson, H. Zhang, H. Xu, *Mol. Brain* **2011**, *4*, 3.
[16] P. Yan, X. Hu, H. Song, K. Yin, R. J. Bateman, J. R. Cirrito, Q. Xiao, F. F. Hsu, J. W. Turk, J. Xu, C. Y. Hsu, D. M. Holtzman, J.-M. Lee, *J. Biol. Chem.* **2006**, *281*, 24566-24574.
[17] J. W. Kinney, S. M. Bemiller, A. S. Murtishaw, A. M. Leisgang, A. M. Salazar, B. T. Lamb, *Alzheimer's Dement.: Transl. Res. Clin. Interv.* **2018**, *4*, 575-590.
[18] D. Giulian, L. J. Haverkamp, J. Yu, W. Karshin, D. Tom, J. Li, A. Kazanskaia, J. Kirkpatrick, A. E. Roher, *J. Biol. Chem.* **1998**, *273*, 29719-29726.
[19] aW. A. Banks, A. Kovac, P. Majerova, K. M. Bullock, M. Shi, J. Zhang, *J. Alzheimers Dis.* **2017**, *55*, 411-419; bW. A. Banks, S. M. Robinson, R. Diaz-Espinoza, A. Urayama, C. Soto, *Exp. Neurol.* **2009**, *218*, 162-167; cY. T. Sui, K. M. Bullock, M. A. Erickson, J. Zhang, W. A. Banks, *Peptides* **2014**, *62*, 197-202.

Entry for the Table of Contents

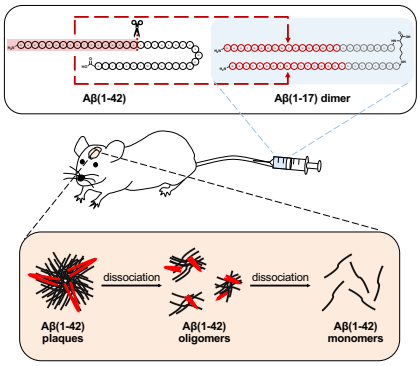

Based on the N-terminal of amyloid-β, we designed a dimeric Aβ(1-17)-based peptide drug that crosses the blood-brain barrier and dissociates amyloid plaques and oligomers upon administration to transgenic Alzheimer model mice.